

Supporting Information

Highly-oriented hybrid microarray modified electrode fabricated by a template-free method for ultrasensitive electrochemical DNA recognition

Lei Shi^a, Zhenyu Chu^a, Xueliang Dong^a, Wanqin Jin^{*a}, and Eithne Dempsey^b

^aState Key Laboratory of Materials-Oriented Chemical Engineering, College of Chemistry and Chemical Engineering, Nanjing University of Technology, 5 Xinmofan Road, Nanjing 210009, P. R. China.

^bCentre for Research in Electroanalytical Technologies (CREATE), Department of Science, Institute of Technology Tallaght, Tallaght, Dublin 24, Ireland

This file includes 7 sections:

1. Four-probe method for determining the conductivity of the hybrid crystal
2. [Stability comparisons of the hybrid films incubated with different crystallization time](#)
3. The effect of different surface coverage of 1,4-benzenedithiol SAMs on the morphologies of obtained hybrid microarray
4. [The electrochemical characterizations of the hybrid films](#)
5. DFT simulations of the 1,6-hexanedithiol and 1,4-benzenedithiol SAMs
6. Calculation of the surface area of the highly oriented hybrid films
7. Regeneration and stability of the fabricated DNA biosensor

1. Four-probe method for determining the conductivity of the hybrid crystal

The four-probe method was performed to detect the conductivity of a single hybrid crystal approximately, which could avoid disturbances of the contact resistance existing in the two-probe method. The resistivity was calculated by the equation (1):

$$\rho = 2\pi S \frac{U}{I} \quad (1)$$

$$\rho = 2 \times 3.14 \times 0.06 \times 2.986 \times 10^3 \text{ } \Omega \cdot \text{cm} = 1.125 \times 10^3 \text{ } \Omega \cdot \text{cm}$$

$$\sigma = \frac{1}{\rho} = 8.9 \times 10^{-4} \text{ S} \cdot \text{m}^{-1}$$

Where ρ is the resistivity, S is the average length between each probe, U is the applied voltage, I is the obtained current and σ represents the conductivity.

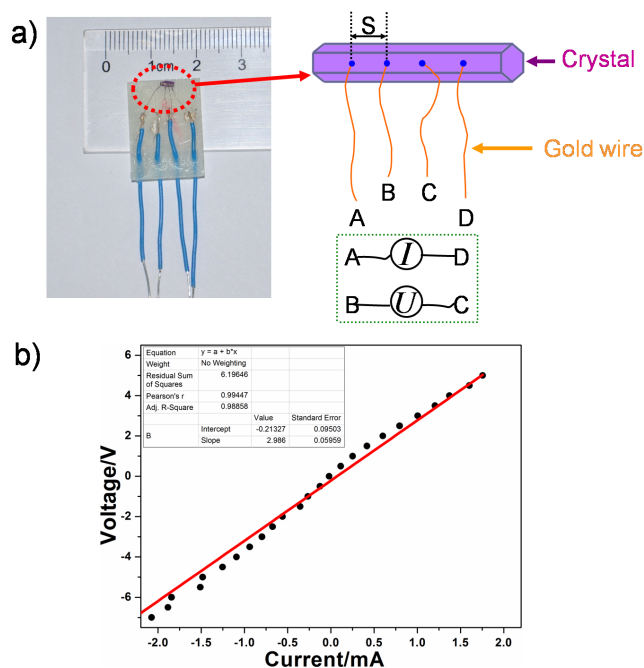


Fig. S1 (a) Photograph (left) and schematic diagram (right) of the four-probe model.

(b) The calibration curve showing voltage versus current, the slope represents the resistance (Ω).

2. Stability comparisons of the hybrid films incubated with different crystallization time

Hybrid films modified electrodes incubated with different crystallization time were shown in Fig. S2. With a crystallization time of 7 h, hexagonal prisms with defects on the surfaces were attained (Fig. S2a), while with more time up to 10 h, a perfect structure of hexagonal prism was obtained (Fig. S2b). When the hybrid films modified electrodes were dipped into the PBS solution for 48 h, the morphology of the hybrid film incubated in the crystallization solution for 7 h changed distinctly (Fig. S2c), while the intact structure of hexagonal prism was kept with subtle changes (Fig. S2d). As the hybrid material consists of the framework of $\{\text{Ag}_2\text{I}_4^{2-}\}_\infty$ and the $\text{Ni}(\text{en})_3^{2+}$ in the cavity, in the case of the intact hybrid crystal, the $\text{Ni}(\text{en})_3^{2+}$ groups may be entirely protected by the stable framework of $\{\text{Ag}_2\text{I}_4^{2-}\}_\infty$, which would be resisted to the PBS solution. However, if the crystal possesses defects on the surface, the $\text{Ni}(\text{en})_3^{2+}$ in the cavity was probable to exposed in the ambient solution, then the ethylenediamine (en) would interact with the ambient solution and finally lead to the complete change in the structure.

In addition, the DNA biosensors based on hybrid films incubated with various crystallization time were regenerated for 6 cycles to investigate the stability of the fabricated sensors. As shown in Fig. S2e, the biosensor based on hybrid microarray with perfect structure could be regenerated with 6 times with about 11.5% loss of the original signal changes. While on the microarray with defects, a significant loss about 76.5% of the original signal changes was observed.

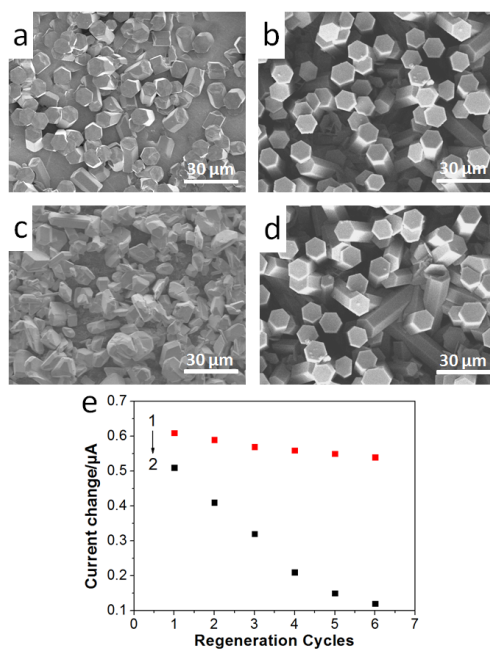


Fig. S2 FESEM images of hybrid films incubated with different crystallization time on 1,4-benzenedithiol modified gold substrates respectively. (a) 7 h, (b) 10 h, (c) 7 h, after dipping in the PBS for 48 h, (d) 10 h, after dipping in the PBS for 48 h. (e) Regeneration tests of the fabricated DNA biosensor based on hybrid films incubated with different crystallization time: (1) 10 h, (2) 7 h.

3. The effect of different surface coverage of 1,4-benzenedithiol SAMs on the morphologies of obtained hybrid microarray

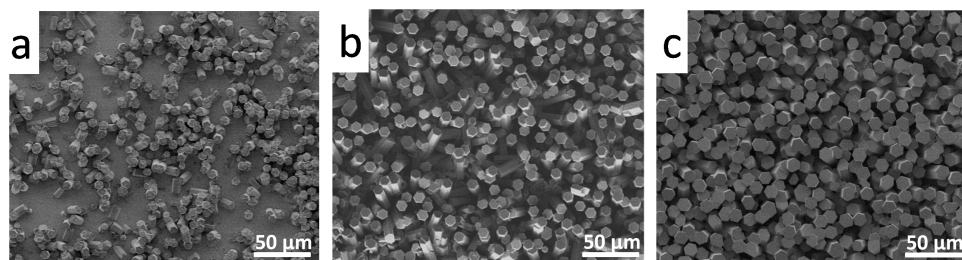


Fig. S3 Hybrid microarray with different distribution densities on the gold substrates modified with the 1,4-benzenedithiol solution for (a) 2 h, (b) 6 h and (c) 10 h respectively.

4. The electrochemical characterizations of the hybrid films

The hybrid microarray modified electrodes with different densities were electrochemically characterized in a 10 mM $\text{K}_3\text{Fe}(\text{CN})_6$ containing 3 M KCl solution at a scan rate of $100 \text{ mV}\cdot\text{s}^{-1}$. As shown in Fig. S4, the results showed that the peak current increased with the immersion time of 1,4-benzenedithiol ranging from 2 h to 6 h, while further increased the immersion time to 10 h, a obvious decline of the peak current was observed. Considering that the surface area of sparse microarray was limited, and the crowded microarray would not facilitate the diffusion profiles, the microarray with moderate density on the gold substrate was selected for constructing the DNA biosensor.

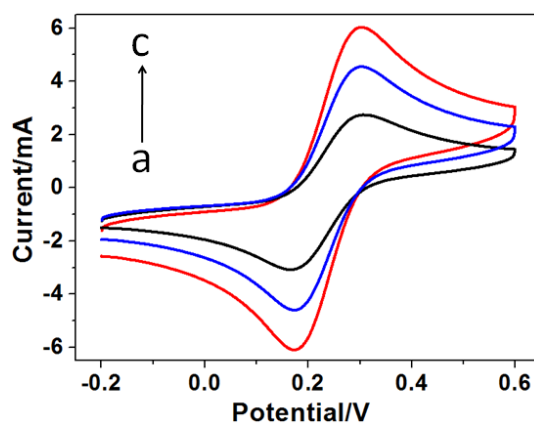


Fig. S4 Cyclic voltammetry curves in 10 mM $\text{K}_3\text{Fe}(\text{CN})_6$ containing 3 M KCl of hybrid microarray with different densities, (a) immersion in the 1,4-benzenedithiol for 2 h, (b) 10 h and (c) 6 h.

5. DFT simulations of the 1,6-hexanedithiol and 1,4-benzenedithiol SAMs

Simulation of SAMs 1,6-hexanedithiol and 1,4-benzenedithiol was performed via Density Functional Theory (DFT). Before the calculation, adsorption models of cell structure were firstly established. The Au surface served as the basic layer to interact with 1,6-hexanedithiol and 1,4-benzenedithiol, and the Au crystal was cleaved to (001) face, then a 20.00 Å vacuum slab was added into (001) face to provide the adsorption space for further molecules inset. After the geometry optimization of 1,6-hexanedithiol and 1,4-benzenedithiol molecules, they were respectively moved into the space of Au surface to complete the construction of simulative models (Fig. S5a, S5c). Finally, the castep package was used to optimize above models for the energy and force minimum. The results from the simulations showed that disordered and flexible 1,6-hexanedithiol SAM was obtained, while employing a rigid 1,4-benzenedithiol led to a significantly improved and relatively erect SAM (Fig. S5b, S5d).

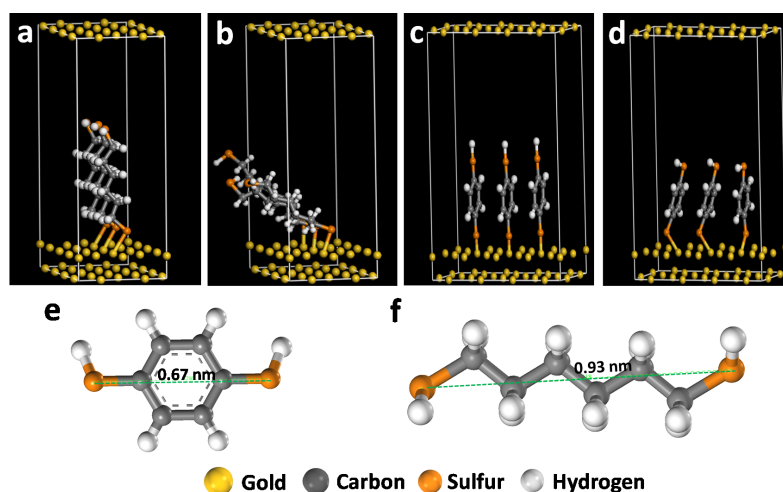


Fig. S5 DFT simulations of 1,6-hexanedithiol SAM (a, before, b, after simulation) and 1,4-benzenedithiol SAM (c, before, d, after simulation). (e) and (f) represented structural formulae of 1,4-benzenedithiol and 1,6-hexanedithiol. The physical lengths of (e) and (f) were 6.7 and 9.3 Å respectively.

6. Calculation of the surface area of highly oriented hybrid films

Here, we assume a simplified picture, in which the dimensions of hexagonal prisms are uniform, namely 25 μm in height, 5 μm in side length (Fig. S6), and the surface area A of oriented films can be calculated by the equation (2). According to the equation, the area A is approximately estimated to be 0.08 cm^2 , which is about ten times greater than that of its macro area, and this large specific area is beneficial for applications in chemical sensing.

$$A = \left[6 \times \text{length} \times \text{height} + \frac{3\sqrt{3}}{2} \times \text{length}^2 \right] \times (\text{number of hexagonal prisms}) \quad (2)$$

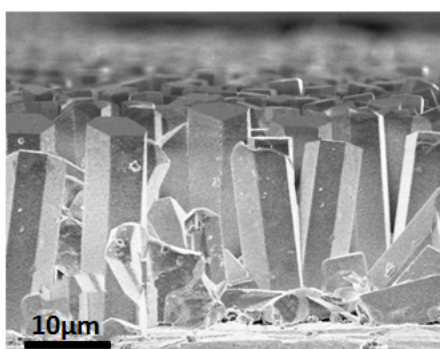


Fig. S6 The cross-section of hybrid microarray on gold surfaces after being immersed in the crystallization solution for 10 h.

7. Regeneration and stability of the fabricated DNA biosensor

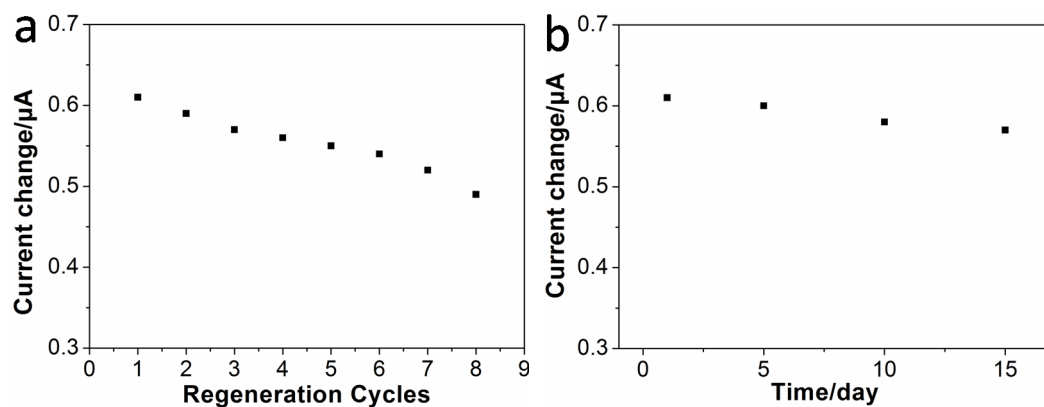


Fig. S7 (a) Regeneration and (b) Stability tests of the hybrid microarray based DNA biosensor, 100 pM of target strands were added each time.